LAWRENCE
LIVERMORE
NATIONAL
LABORATORY

LLNL-CONF-412951

Morphology, microstructure, stress and damage properties of thin film coatings for the LCLS x-ray mirrors

R. Soufli, S. L. Baker, J. C. Robinson, E. M. Gullikson, T. J. McCarville, M. J. Pivovaroff, P. Stefan, S. P. Hau-Riege, R. Bionta

May 12, 2009

Damage to VUV, EUV and X-ray Optics II, SPIE Europe Optics and Optoelectronics
Prague, Czech Republic
April 20, 2009 through April 23, 2009

Disclaimer

Morphology, microstructure, stress and damage properties of thin film coatings for the LCLS x-ray mirrors

Regina Soufli[1*], Sherry L. Baker[1], Jeff C. Robinson[1], Eric M. Gullikson[2], Tom J. McCarville[1], Michael J. Pivovaroff[1], Peter Stefan[3], Stefan P. Hau-Riege[1], Richard Bionta[1]

[1]Lawrence Livermore National Laboratory, 7000 East Avenue, Livermore, CA 94550, US
[2]Lawrence Berkeley National Laboratory, 1 Cyclotron Road, Berkeley, CA 94720, US
[3]SLAC National Accelerator Laboratory, 2575 Sand Hill Road, Menlo Park, CA 94025, US

ABSTRACT

The development and properties of reflective coatings for the x-ray offset mirror systems of the Linac Coherent Light Source (LCLS) free-electron laser (FEL) are discussed in this manuscript. The uniquely high instantaneous dose of the LCLS FEL beam translates to strict limits in terms of materials choice, thus leading to an x-ray mirror design consisting of a reflective coating deposited on a silicon substrate. Coherent wavefront preservation requirements for these mirrors result in stringent surface figure and finish specifications. DC-magnetron sputtered B_4C and SiC thin film coatings with optimized stress, roughness and figure properties for the LCLS x-ray mirrors are presented. The evolution of microstructure, morphology, and stress of these thin films versus deposition conditions is discussed. Experimental results on the performance of these coatings with respect to FEL damage are also presented.

Keywords: free-electron lasers, x-ray optics, boron carbide, silicon carbide

1. INTRODUCTION

The Linac Coherent Light Source (LCLS) FEL is currently being constructed at the Stanford Linear Accelerator Center (SLAC). LCLS is anticipated to begin operation in 2009, and will be the first x-ray FEL facility in the world in the 0.827 to 8.27 keV photon energy region (0.15 − 1.5 nm wavelength region). The unprecedented brightness, coherence, and resolution properties of the LCLS will enable tremendous advances in the fields of biology, physics, and materials sciences. The experimental areas planned for the LCLS, each with its own dedicated end-station (hutch), include: soft x-ray research (SXR); atomic, molecular and optical science (AMO); x-ray pump-probe (XPP); x-ray photon correlation spectroscopy (XPCS); coherent x-ray imaging (CXI); and materials under extreme conditions (MEC)[1]. The layout of the LCLS facility, including the experimental end-stations, has been discussed in detail in an earlier SPIE Proceedings publication[2]. The LCLS x-ray mirror systems serve two distinct purposes. The first is to dramatically reduce the amount of high-energy spontaneous radiation, bremsstrahlung γ-rays and their secondary products within the experimental hutches. The second is to physically separate the FEL beam from the spontaneous, broad-band undulator radiation that would contaminate the spectrally-pure, coherent FEL radiation. An elegant method for achieving the desired goals relies on grazing-incidence mirrors to act as a low-pass energy filter, efficiently reflecting and deflecting the FEL beam to a trajectory slightly offset from the primary axis of the LCLS facility. To minimize costs associated with translating experiments out of the FEL path, allowing the FEL beam to pass to another hutch further down stream, the LCLS x-ray mirror system is designed to provide several different branch lines. The initial LCLS configuration will contain three "lines" by using a combination of fixed and moveable reflective mirrors and splitting the 0.827−8.27 keV first-harmonic range into two regimes: a 0.827−2.00 keV soft x-ray band and a 2.00−8.27 keV hard x-ray band. As has been described in detail in References. 2, 3, a total of four mirrors will create two soft x-ray branches, the Soft X-ray Offset Mirror System (SOMS), that will deliver X-rays to the SXR and AMO hutches. Two additional mirrors will form the Hard X-ray Offset Mirror System (HOMS), and will create the single hard x-ray branch line that will initially deliver photons to

* e-mail: regina.soufli@llnl.gov, phone: 925-422-6013

the XPP and CXI hutches. Our group at Lawrence Livermore National Laboratory (LLNL) has led a team composed of national labs and industry in the design, specification, fabrication and precision surface metrology of the LCLS SOMS and HOMS mirror systems.

The LCLS physics requirements that drive the specifications for the SOMS and HOMS LCLS x-ray mirrors mirrors have been discussed in detail in References 2, 3 (and references therein) and are related to:

1. *Reflective materials specifications:* One of the most unique LCLS beam properties is the extremely high peak brightness (~ 10^{32} photons*sec^{-1}*mm^{-2}*mrad^{-2} *(0.1% bandwidth)$^{-1}$), which is over ten orders of magnitude higher than current third-generation synchrotron sources. Earlier studies[4,5,6,7] indicated that only a few low-Z materials (Be, B_4C, SiC and Al_2O_3) would be expected to survive the peak brightness of the LCLS FEL beam after it leaves the undulator enclosure. In addition, there is a requirement for absence of absorption edges in the photon energy range of operation (0.827−2.00 keV for the SOMS mirrors and 2.00−8.27 keV for the HOMS mirrors), to ease the calibration of reflectivity data obtained from the mirrors.
2. *3rd harmonic rejection:* The reflectance of each SOMS mirror at photon energies above 2.48 keV should be less than 20%.
3. *Mirror reflectance:* Each mirror should have reflectivity ≥ 90% in the entire photon energy range of operation at the grazing angle of incidence of 13.85 mrad for the SOMS mirrors and 1.38 mrad for the HOMS mirrors
4. *Mirror geometry:* The mirrors will have flat, planar reflective surfaces
5. *Mirror acceptance:* Each mirror should be sized to accept at least 95% of the FEL beam radiation cone.
6. *Mirror surface specifications:* Each mirror surface should be specified to limit degradation of the transverse coherence of the FEL beam. In addition, each mirror should not reduce the FEL beam intensity by more than 20% or broaden its divergence by more than 10%.

Requirements no. 1, 2 and 3 above, combined with the state-of-the-art in vendor capabilities to polish/figure specific materials, resulted in a design for the SOMS mirrors consisting of a Si substrate followed by a 50-nm thick B_4C reflective coating, and a design for the HOMS mirrors consisting of a Si substrate followed by a 50-nm thick SiC reflective coating. Requirements no. 4, 5, 6 above, resulted in the surface figure, mid-spatial frequency roughness (MSFR) and high-spatial frequency roughness (HSFR) specifications summarized in Table 1. The size of the SOMS mirror was defined as 250 mm (length)×30 mm (width) ×50 mm (height), with a clear aperture (illuminated area required to meet surface specifications) of 175 mm ×10 mm. The size of the HOMS mirror was defined as 450 mm (length)×30 mm (width) ×50 mm (height), with a clear aperture of 385 mm ×15 mm. The slope and height error specifications in Table 1 apply to the tangential direction, after subtraction of any spherical-term figure error component. The mirror surface figure is especially crucial in meeting the requirements for coherence preservation of the LCLS FEL beam. Achieving the surface specifications for the mirror substrate figure and finish in Table 1 is a daunting task and is truly pushing the limits of the state-of-the-art in Si substrate manufacturing and metrology. Surface metrology results from the SOMS Si substrates are discussed in detail in Ref. 3. The mounting design and other opto-mechanical and thermal considerations for the SOMS mirrors are discussed in detail in Ref. 8.

Error Category		Specification	Spatial Wavelength
Figure	Height Error	≤ 2.0 nm rms	1 mm to Clear Aperture
	Slope Error	≤ 0.25 μrad rms	
MSFR		≤ 0.25 nm rms	2 μm to 1 mm
HSFR		≤ 0.4 nm rms	20 nm to 2 μm

Table 1: Surface specifications for the figure, MSFR and HSFR of the SOMS and HOMS Si substrates. All specifications are applicable within the substrate clear aperture area, 175mm × 10 mm (SOMS mirrors) and 385 mm × 15 mm (HOMS mirrors).

One of the most important requirements for the 50 nm-thick B_4C reflective coating for the LCLS SOMS mirrors and the 50-nm thick SiC coating for the LCLS HOMS mirrors is to preserve the figure of the Si substrate specified in Table 1. Given that the figure errors of the substrate and subsequent reflective coating are uncorrelated and thus add in a quadratic fashion, the thickness variation of the B_4C (or SiC) film should be < 1 nm rms (i.e: about half of the substrate figure specification) across the 175-mm length of SOMS (or 385-mm length of HOMS) mirror clear aperture, in order for the B_4C (or SiC) coating thickness variation to not have a significant contribution to degradation of the mirror figure. Moreover, the coating is required to preserve the MSFR of the Si substrate specified in Table 1. The coating contribution to HSFR should allow for about ≥ 90% reflectance per mirror, as is specified in Section 1. The stress of the coating should be sufficiently low (≤ 1 GPa, for a 50-nm thick coating) to prevent delamination from the substrate and to maintain the overall figure deformation of the coated mirror within the specification of 2 nm rms. As is the case with all reflective coatings for x-ray optics, the top surface of the B_4C (or SiC) film should be stable against contamination (oxidation, hydrocarbons), to maintain consistent reflective performance over time. Experimental results on the SOMS B_4C coatings and HOMS SiC coatings addressing all the above properties and requirements are presented in Sections 2 and 3 of this manuscript, respectively. Experimental results on damage properties of SiC and B_4C coatings are discussed in Section 4.

2. BORON CARBIDE REFLECTIVE COATINGS FOR THE LCLS SOMS MIRRORS

As is discussed in Section 1, B_4C was chosen as the reflective coating material for the LCLS SOMS mirrors mainly due to the predicted high damage threshold against the LCLS FEL beam compared to other coating materials, combined with the good reflective performance and absence of electronic absorption edges in the 0.827-2.00 keV SOMS energy range of operation. For the SOMS mirrors operating at 13.85 mrad grazing incidence angle, it was determined through modeling that the optimum thickness of the B_4C coating is about 50 nm, to ensure good reflective properties and adequate suppression of the higher harmonics of the FEL beam. Although there is significant literature on sputtered B_4C (in the sub-nm to nm thickness range) used as barrier or constituent layer for EUV/x-ray multilayer coatings, there is only limited prior work[9,10,11,12] on the physical and optical properties of single-layer, sputtered B_4C films in the 50-nm thickness range as EUV/x-ray reflective coatings. Specifically in the SOMS photon energy range of operation (0.827-2.00 keV), the experimental reflectance properties of grazing incidence x-ray mirrors with such B_4C coatings have not been investigated previously, until our recent work on the SOMS mirror coatings[3].

B_4C coatings with thickness in the 50-nm range were deposited at LLNL on (100)-orientation Si wafer substrates with nearly ideal HSFR (about 0.05 nm rms). A planar DC-magnetron sputtering system for large-area, ultra-precise EUV/x-ray coatings[13] was used for these depositions. The same system was ultimately used for the deposition of B_4C coatings on the actual SOMS mirror substrates. The stress of a B_4C film made using nominal deposition parameters (1 mTorr pressure of the Ar processing gas) was -2.3 GPa (compressive), which was deemed quite severe but was anticipated, since B_4C is known as one of the most compressively stressed materials in the literature. Although no delamination or other degradation has been observed on several such B_4C films aged for over three years after deposition, this level of coating stress was considered a risk for the actual SOMS mirrors. By especially modifying the deposition parameters (increasing the Ar sputtering pressure to10 mTorr), ~50-nm thick B_4C films with lower stress by a factor of 2 (-1.1 GPa) were produced. Although other techniques exist for stress mitigation (such as introducing compensating layers of different materials, etc), this method was chosen because it maintains the original B_4C film stoichiometry and does not involve other materials, which could be a concern for the damage-resistance of these coatings to the high instantaneous dose of the LCLS. The HSFR (in the spatial frequency range specified in Table 1) of the aforementioned B_4C coatings was measured by Atomic Force Microscopy (AFM). A Digital Instruments Dimension 5000™ AFM instrument was used in the measurements, equipped with an acoustic hood and vibration isolation, resulting in a noise level of 0.03 nm rms. The instrument is operated in tapping mode which measures topography in air by tapping the surface with an oscillating probe tip. The probe tips were etched silicon, with a nominal tip radius of 5-10 nm. AFM scans of 2×2 μm^2 and 10×10 μm^2 were performed and the data from each scan were stored in a 512×512 pixel array. Figure 1 shows a 500×500 nm^2 detail from the 2×2 μm^2 AFM images obtained on each of the two ~50-nm thick B_4C films. The AFM images indicate an increase in roughness, demonstrated as an increase in the size of the grains of the B_4C films, between the two sputtering pressures. This change in morphology between the lower sputtering pressure (1mTorr) and higher sputtering pressure (10 mTorr) B_4C films is consistent with a "zone 1/zone T" structure model proposed by Thornton[14]. According to this model, in the low-temperature regime which is applicable for these B_4C films, the working gas (Ar)

pressure during film deposition is one of the major factors determining the energy and momentum delivered to the surface by the sputtered species. A simplified way to explain the relationship between gas pressure and film roughness would be to think that lower sputtering gas pressures result in fewer collisions/scattering between the sputtered material and the working gas species, thus resulting in higher average energy of the sputtered material upon arrival on the substrate surface, and in deposition angles close to the normal direction from the substrate surface. This regime allows the arriving species to efficiently "arrange" themselves on the film surface, resulting in lower roughness. The reduction in compressive stress of the 10 mTorr film compared to the 1 mTorr film can also be explained using the same phenomenology, including the "atomic peening" effect of energetic particles on the growing film[15]: lower process gas pressures result in bombardment of the film surface by highly energetic particles (atomic peening), resulting in the growth of compact films with compressive stress. Higher process gas pressures cause less atomic peening, resulting in less compact films containing a larger number and size of atomic-scale voids, as is evident in the AFM images in Figure 1. Through these voids the compressive stress can relax towards the tensile direction[16], as is the case between the two B_4C films discussed in this manuscript. Large-angle x-ray diffraction measurements were performed on both B_4C films and characteristic crystalline peaks were not found, indicating amorphous structure. Figure 2 shows the Power Spectral Density (PSD) curves from the two types of B_4C films deposited under two different Ar pressure conditions. The power spectral density (PSD) was computed[17] from the height data in each of the 2×2 μm^2 and 10×10 μm^2 AFM scans obtained on each film. Each PSD curve was formed by first calculating a two-dimensional Fourier power spectrum of the height data, and the spectrum was then averaged azimuthally around zero spatial frequency to produce a PSD with purely radial spatial frequency dependence. This approach works well for quasi-isotropic surfaces, such as the B_4C films discussed in this manuscript. The PSD curves in Figure 2 illustrate the roughness evolution vs. spatial frequency for each of the two B_4C films. The root-mean-square (rms) roughness σ is obtained by the expression

$$\sigma^2 = \int_{f_1}^{f_2} 2\pi f S(f) df \quad , \qquad (1)$$

where f is the spatial frequency, $S(f)$ is the surface PSD, and f_1, f_2 define the spatial frequency range of interest. For the HSFR, where $f_1 = 5\times10^{-4}$ nm^{-1} and $f_2 = 5\times10^{-2}$ nm^{-1} as defined in Table 1, σ was computed according to eq. (1) by combining PSD curves from 10×10 μm^2 and 2×2 μm^2 AFM scans. The intrinsic HSFR of the B_4C film deposited under nominal conditions (1 mTorr Ar pressure) was found to be 0.15 nm rms, while the HSFR of the B_4C film deposited at 10 mTorr was 0.47 nm rms. A comprehensive study of the morphology and stress evolution of B_4C films across a wide range of sputtering pressure and film thickness settings will be given in an upcoming publication.[18]

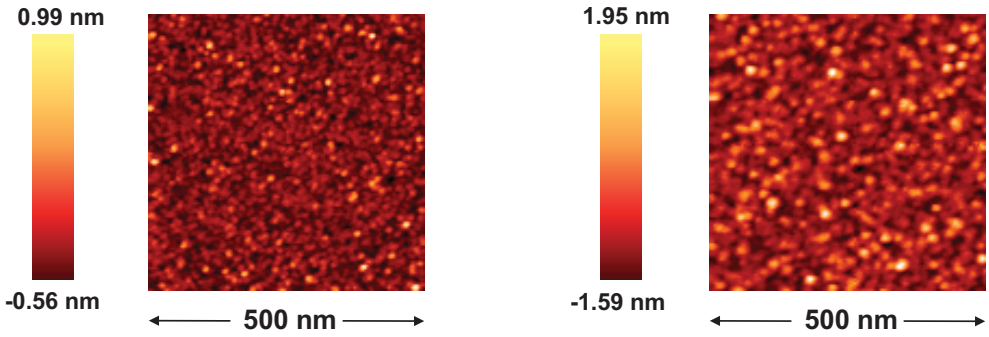

Figure 1: A 500 ×500 nm^2 detail is shown from the 2×2 μm^2 AFM scans obtained on a 56.5 nm –thick B_4C film deposited at 1 mTorr Ar sputtering pressure (left) and a 54.2 nm –thick B_4C film deposited at 10 mTorr Ar sputtering pressure (right). The measured HSFR was 0.15 nm rms (left) and 0.47 nm rms (right). The measured film stress was -2.3 GPa (left) and -1.1 GPa (right). See also Figure 2.

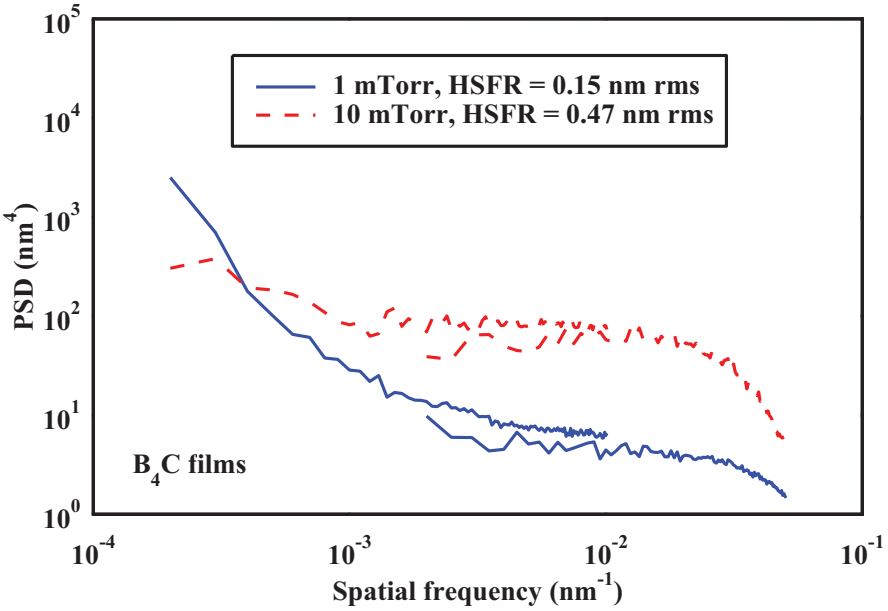

Figure 2: PSD curves and HSFR values derived from 2×2 and 10×10 μm^2 AFM data for a 56.5 nm-thick B_4C film deposited at 1 mTorr and a 54.2 nm-thick B_4C film deposited at 10 mTorr Ar sputtering pressure. See also Figure 1.

To verify the B_4C film composition, Rutherford backscattering (RBS) measurements were performed on B_4C films deposited at both 1 mTorr and 10 mTorr Ar sputtering pressure. The RBS measurements indicated atomic ratio boron:carbon = 3.7:1, with 6% (atomic) oxygen present, averaged across the entire film thickness. The boron:carbon ratio is very close to the prescribed stoichiometry (4:1) of the sputtering target material and the overall composition (including the oxygen content) is consistent with earlier results reported in the literature for sputtered B_4C thin films[19,20,21,22,23,24,25,26]. It was determined that the source of the 6% oxygen in the films is most likely the B_4C sputtering target (i.e: oxygen was incorporated during target fabrication), as opposed to oxygen being present in the environment during deposition. This is further supported by the observation that films of other materials made in the same deposition chamber under similar conditions and tested by RBS show only a fraction of a percent atomic oxygen concentration. Through the RBS measurements it was also determined that the density of the sputtered B_4C films is 2.28 g/cm^3, which corresponds to 90% of the bulk density of a B_4C crystal (2.52 g/cm^3). The RBS analysis results were identical for B_4C films deposited at both 1 mTorr and 10 mTorr Ar sputtering pressures. Since the chemical composition of the top surface of a reflective film used at grazing angles of incidence is crucial in the understanding of its x-ray reflectance properties, X-ray Photoelectron Spectroscopy (XPS) was also performed. XPS on a B_4C sample deposited at 10 mTorr and aged for about one month indicated that the top 9 nm of the film are oxygen- and carbon- rich (boron=64%, carbon= 22%, oxygen=13%, atomic) with the oxygen and carbon concentrations rapidly diminishing with increasing depth from the top surface. RBS and XPS measurements were performed by Evans Analytical Group (Sunnyvale, California). The refractive index (optical constants) of the B_4C films was also determined experimentally via photoabsorption measurements in the 30-770 eV photon energy range, performed at beamline 6.3.2 of the Advanced Light Source (ALS) synchrotron at Lawrence Berkeley National Laboratory (LBNL). The measurements resulted in updated values for the optical constants of sputtered B_4C, and NEXAFS structure was revealed in the vicinity of the boron, carbon and oxygen K edge energy regions[27].

The 50-nm thick B_4C film with 0.47 nm intrinsic HSFR and -1.1 GPa stress was ultimately selected as the optimum coating for the LCLS SOMS mirrors, due to the significantly lower stress of this modified B_4C film, as explained above. As is also discussed in detail in Ref. 3, this B_4C film meets the x-ray reflectance requirements discussed in Section 1, and has been predicted -and experimentally verified- to induce a figure deformation with a spherical-term-like shape on the SOMS substrate, which can be corrected using a special bending mechanism during final assembly of the SOMS mirrors[8]. Ref. 3 also discusses the HSFR evolution of the SOMS B_4C coating on a substrate with arbitrary roughness, and HSFR prediction using a stochastic thin film growth model[28]. It was found that the B_4C coating affects the HSFR for spatial frequencies greater than 2×10^{-3} nm^{-1}. In the rest of the HSFR and in the MSFR ranges, the B_4C coating

replicates the topography of the Si substrate, as has also been demonstrated on earlier DC-magnetron sputtered coatings of various single-layer and multilayer materials deposited under similar conditions[29,30]. In Ref. 3, a test Si subsrate with HSFR = 0.36 nm rms was coated with a B_4C film using the SOMS deposition parameters. The HSFR of the B_4C-coated top surface was measured at 0.79 nm rms. Since the measured HSFR of the SOMS Si substrates that have been chosen for installation is in the 0.3-0.5 nm rms range (i.e: close to the HSFR of the Si test substrate mentioned above), the HSFR of the B_4C coated Si substrate should be representative of the SOMS mirrors. All SOMS Si substrates have been delivered and characterized by precision surface metrology at LLNL, and the B_4C depositions for SOMS mirrors have been completed. Using a special methodology developed for the SOMS mirrors and discussed in detail in Ref. 3, the thickness variation of the B_4C coating across the SOMS 175 mm-long CA was minimized, and resulted in a coating-added figure error of < 0.14 nm rms[3], which is well within the 1 nm rms specification discussed in Section 1. Initial post-coating interferometry results on the SOMS mirrors confirm that the B_4C coating indeed does not affect the overall figure error.

3. SILICON CARBIDE REFLECTIVE COATINGS FOR THE LCLS HOMS MIRRORS

In a manner similar to the selection of B_4C for SOMS, SiC was chosen as the reflective coating material for the LCLS HOMS mirrors mainly due to the predicted high damage threshold against the LCLS FEL beam compared to other coating materials, combined with the good reflective performance and absence of electronic absorption edges in the 2.00-8.27 keV HOMS energy range of operation. For the HOMS mirrors operating at 1.35 mrad grazing incidence angle, the optimum thickness of the SiC coating was also found to be 50 nm, to ensure that the reflective requirements in Section 1 are met. SiC coatings with thicknesses in the 50-nm range were deposited at LLNL on (100)-orientation Si wafer substrates with nearly ideal HSFR (about 0.05 nm rms), using the deposition system discussed in Section 2, which was also used for the deposition of SiC coatings on the actual HOMS mirror substrates. The stress of a SiC film made using nominal deposition parameters (1 mTorr Ar pressure) was -1.7 GPa. Although lower than the -2.3 GPa stress measured for the B_4C films deposited at 1 mTorr as discussed in Section 2, this level of coating stress was still considered a risk for the actual HOMS mirrors. By increasing the Ar sputtering pressure to 3 mTorr, ~50-nm thick SiC films with lower stress by a factor of 2 (-0.8 GPa) were produced. The HSFR (in the frequency range specified in Table 1) of the aforementioned SiC coatings was measured by AFM, using the same instrument and methodology presented in Section 2. Figure 3 shows the Power Spectral Density (PSD) curves from the two types of SiC films deposited under two different Ar pressure conditions.

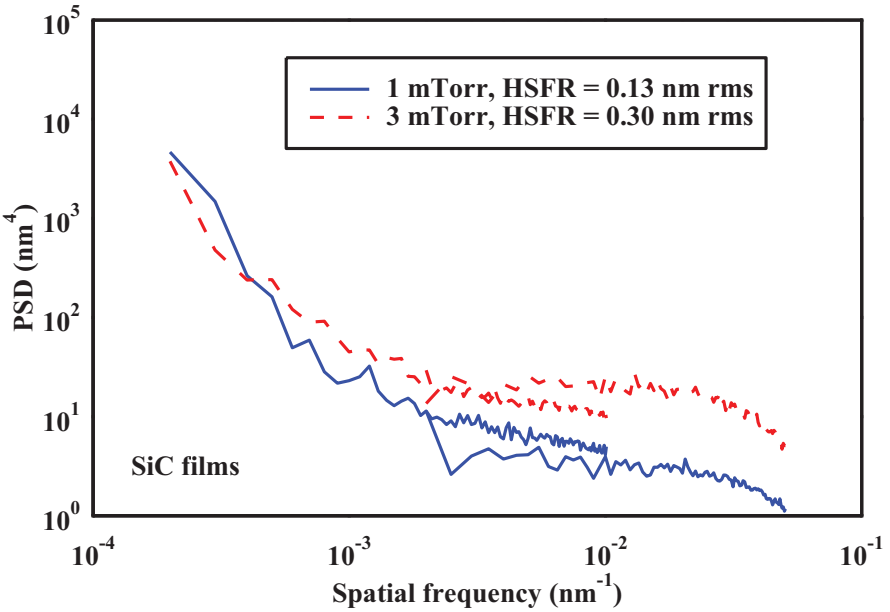

Figure 3: PSD curves and HSFR values derived from 2×2 and 10×10 μm^2 AFM data for a 46.3 nm-thick SiC film deposited at 1 mTorr and a 53.4 nm-thick SiC film deposited at 3 mTorr Ar sputtering pressure.

The intrinsic HSFR of the SiC film deposited under nominal conditions (1 mTorr Ar pressure) was found to be 0.13 nm rms, while the HSFR of the SiC film deposited at 3 mTorr was 0.30 nm rms. The change in morphology and the trend of lower stress and increased HSFR with increasing Ar sputtering pressure for these SiC films can be understood with the mechanisms and models discussed in Section 2. RBS measurements were also performed on SiC films deposited at 3mTorr Ar sputtering pressure. The RBS measurements indicated atomic ratio silicon:carbon = 1:1.04, with 5% (atomic) oxygen present, averaged across the entire film thickness. The silicon:carbon ratio is very close to the prescribed stoichiometry (1:1). The source of the 5% oxygen in the films is most likely the SiC sputtering target (i.e: oxygen was incorporated during target fabrication), as was also discussed in Section 2.Through the RBS measurements it was also determined that the density of the sputtered SiC films is 2.98 g/cm^3, corresponding to 94% of the bulk density of a SiC crystal (3.17 g/cm^3). The 50-nm thick SiC film with 0.30 nm rms intrinsic HSFR and -0.8 GPa stress deposited at 3 mTorr was ultimately selected as the optimum coating for the LCLS HOMS mirrors, due to the significantly lower stress and relatively low HSFR of this modified SiC film. The HOMS Si substrates are currently being delivered and characterized by precision surface metrology at LLNL, and the SiC depositions for HOMS mirrors are underway. Using the methodology discussed in detail in Ref. 3, the thickness variation of the SiC coating across the HOMS 385 mm-long clear aperture was minimized experimentally, and resulted in a coating-added figure error < 0.34 nm rms, well within the 1 nm rms specification discussed in Section 1.

4. FEL DAMAGE OF BORON CARBIDE AND SILICON CARBIDE THIN FILM COATINGS

We define damage as anything that can cause degradation or failure of an optic. Possible damage mechanisms include melting, phase change, high-pressure effects such as spallation or shear, thermal stress and fatigue, and photochemical processes. Theoretical analyses of x-ray processes and experience from optical laser-matter interaction studies suggest that the expected damage threshold is at or substantially below the melt threshold. Low-Z materials with high melting points are expected to exhibit a high damage resistance since they absorb less, so that the energy density is smaller, and they are mechanically stable. Since x-ray FELs are not available yet, we have performed single-pulse damage experiments on existing light sources, including the EUV FEL FLASH in Hamburg, Germany. We found that the damage threshold in bulk B_4C and SiC samples is somewhat higher than the expected melt threshold[7], which supports the main tenet for designing the x-ray optics with B_4C and SiC coatings. Furthermore, we found the single-pulse damage threshold in thin films generally to be smaller than for bulk materials, and that the damage thresholds increase for shorter wavelengths between 32 and 13.5 nm[31]. We also performed multiple-pulse damage experiments on B_4C thin films, using the temperature profile in the structure as the point of comparison to the XFEL case. In these experiments we found the single-pulse film damage threshold to be about two times lower than the value we found in the FLASH experiments, and the multiple-pulse film damage threshold was lower by another factor of two to three[32]. Figure 4 summarizes the aforementioned results. All the damage doses we found in the experiments are significantly higher than the doses that are expected to occur in the SOMS and HOMS mirror systems at LCLS.

5. SUMMARY AND FUTURE WORK

The LCLS SOMS and HOMS x-ray mirror systems have been designed and constructed, and B_4C and SiC reflective coatings have been developed for the SOMS and HOMS Si substrates respectively. Each coating has been especially optimized and modified to satisfy stringent requirements for low stress, high reflectance and coherent wavefront propagation of the LCLS beam. We have ongoing research towards better understanding of thin film and mirror substrate damage properties under peak power FEL conditions. We have also incorporated precision metrology results obtained at LLNL on SOMS and HOMS mirrors into first-principles wavefront propagation models for the LCLS beam, and have predicted the LCLS focal spot structure; we will report on these results in upcoming publications[33].

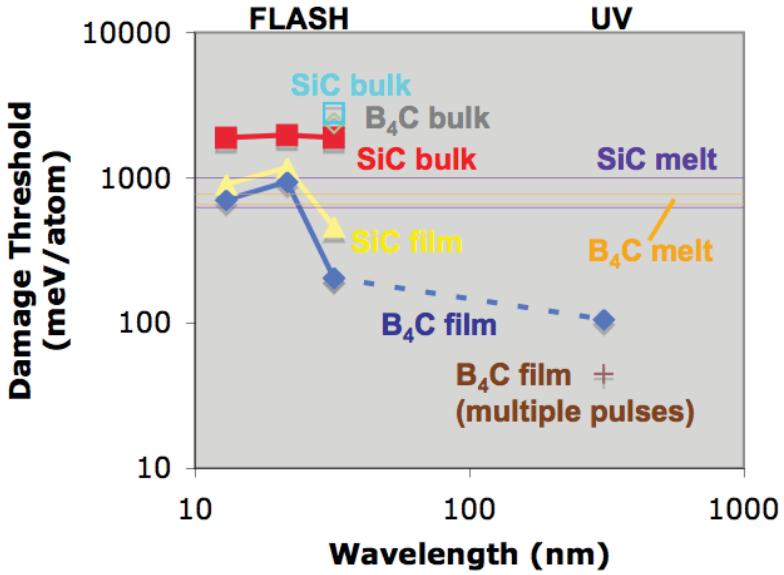

Figure 4: A summary of damage experiment results on B_4C and SiC films is plotted. The damage experiments were performed in the EUV wavelength region (FLASH facility, single-shot exposures) and at 308 nm (excimer laser, multiple-shot exposures)[7, 31,32]. The theoretical B_4C and SiC melt thresholds are shown as horizontal lines.

ACKNOWLEDGEMENTS

We are grateful to Donn McMahon (LLNL) and to the LCLS executive management at SLAC for project support. We thank Angela Craig, Bruce Rothman and Patrick Schnabel (Evans Analytical Group, Sunnyvale, California) for the XPS and RBS measurements. This work performed under the auspices of the U.S. Department of Energy by Lawrence Livermore National Laboratory under Contract DE-AC52-07NA27344. Work was supported in part by DOE Contract DE-AC02-76SF00515. This work was performed in support of the LCLS project at SLAC.

REFERENCES

[1] The LCLS Design Study Group, "Linac coherent light source (LCLS) design study report." SLAC-R-521; UC-414; http://www-ssrl.slac.stanford.edu/lcls/design report/e-toc.html, December 1998.
[2] M. Pivovaroff, R. M. Bionta, T. J. Mccarville, R. Soufli, P. M. Stefan, "Soft X-ray mirrors for the Linac Coherent Light Source", Proc. SPIE **6705**, 67050O (2007).
[3] R. Soufli, M. J. Pivovaroff, S. L. Baker, J. C. Robinson, E. M. Gullikson, T. J. McCarville, P. M. Stefan, A. L. Aquila, J. Ayers, M. A. McKernan, R. M. Bionta, "Development, characterization and experimental performance of x-ray optics for the LCLS free-electron laser" Proc. SPIE **7077,** 707716 (2008).
[4] R. M. Bionta, "Controlling dose to low-Z solids at LCLS." LLNL report: UCRL-ID-137222; http://www.llnl.gov/tid/lof/documents/pdf/237970.pdf , Jan 2000.
[5] D. D. Ryutov, "Thermal stresses in the reflective x-ray optics for the linac coherent light source," *Rev Sci Inst* **74**, 3722–3725 (2003).
[6] S. Hau-Riege, "Absorbed XFEL dose in the components of the LCLS X-Ray optics." LLNL report: UCRLTR-215833; http://www.llnl.gov/tid/lof/documents/pdf/325503.pdf, October 2005.
[7] S. P. Hau-Riege, R. A. London, R. M. Bionta, M. A. McKernan, S. L. Baker, J. Krzywinski, R. Sobierajski, R. Nietubyc, J. B. Pelka, M. Jurek, L. Juha, J. Chalupsky, J. Cihelka, V. Hajkova, A. Velyhan, J. Krasa, J.Kuba, K. Tiedtke, S. Toleikis, T.Tschentscher, H. Wabnitz, M. Bergh, C. Caleman, K. Sokolowski-Tinten, N. Stojanovic, and U. Zastrau, "Damage threshold of inorganic solids under free-electron-laser irradiation at 32.5 nm wavelength," *App. Phys. Lett.* **90**, 173128 (2007).
[8] T. J. McCarville, P. M. Stefan, B. Woods, R. M. Bionta, R. Soufli, M. J. Pivovaroff, "Opto-mechanical design considerations for the Linac Coherent Light Source X-ray mirror system", Proc. SPIE **7077** 70770E (2008).

[9] G. M. Blumenstock and Ritva A. M. Keski-Kuha, "Ion-beam-deposited boron carbide coatings for the extreme ultraviolet", Appl. Opt. **33**, 5962-5963 (1994).
[10] G. M. Blumenstock, R. A. M. Keski-Kuha, and M. L. Ginter, "Extreme ultraviolet optical properties of ion-beam-deposited boron carbide thin films", Proc. SPIE **2515**, 558-564 (1995).
[11] C. Tarrio, R. N. Watts, T. B. Lucatorto, J. M. Slaughter, and C. M. Falco, "Optical constants of *in situ*-deposited films of important extreme-ultraviolet multilayer mirror materials", Appl. Opt. **37** 4100-4104 (1998).
[12] J. I. Larruquert and R. A. M. Keski-Kuha, "Optical properties of hot-pressed B4C in the extreme ultraviolet", Appl. Opt. **39**, 1537-1540 (2000).
[13] R. Soufli, R. M. Hudyma, E. Spiller, E. M. Gullikson, M. A. Schmidt, J. C. Robinson, S. L. Baker, C. C. Walton, and J. S. Taylor "Sub-diffraction-limited multilayer coatings for the 0.3 numerical aperture micro-exposure tool for extreme ultraviolet lithography", Appl. Opt. **46**, 3736-3746 (2007).
[14] J. A. Thornton, "The micro-structure of sputter-deposited coatings"J. Vac. Sci. Technol. A **4**, 3059-3065 (1986).
[15] F. M. d'Heurle, "Aluminum films deposited by rf sputtering", Metall. Trans **1**, 725 (1970).
[16] T. J. Vink, W. Walrave, J. L. C. Daams, A. G. Dirks, M. A. Somers, K. J. A. van der Aker, "Stress, strain, and microstructure in thin tungsten films deposited by dc magnetron sputtering", J. App. Phys. **74**, 988-995 (1993).
[17] D. L. Windt, "topo - surface topography analysis", available at http://www.rxollc.com/idl/index.html
[18] R. Soufli, S. L. Baker, J. C. Robinson, E. M. Gullikson, R. M. Bionta, "Morphology, microstructure and stress evolution of magnetron sputtered boron carbide thin films for extreme ultraviolet / x-ray applications", to be submitted to the Journal of Applied Physics.
[19] G. M. Blumenstock, R. A. M. Keski-Kuha, and M. L. Ginter, "Extreme ultraviolet optical properties of ion-beam-deposited boron carbide thin films", Proc. SPIE **2515**, 558-564 (1995).
[20] M.-L. Wu, J. D. Kiely, T. Klemmer, Y.-T. Hsia, K. Howard, "Process-property relationship of boron carbide thin films by magnetron sputtering" Thin Solid Films **449**, 120-124 (2004).
[21] T. Hu, L. Steihl, W. Rafaniello, *et al*, "Structures and properties of disordered boron carbide coatings generated by magnetron sputtering", Thin Solid Films **332**, 80-86 (1998).
[22] C. I. Chiang, H. Holleck and O. Meyer, "Properties of RF sputtered B_4C thin films", NIM B **91**, 692-695 (1994).
[23] C. I. Chiang, O. Meyer, Rui M. C. da Silva, "The modification of mechanical properties and adhesion of boron carbide sputtered films by ion implantation", NIM B **117**, 408-414 (1996).
[24] E. Pascual, E. Martinez, J. Esteve, A. Lousa, "Boron carbide thin films deposited by tuned-substrate RF magnetron sputtering", Diamond and Related Materials **8**, 402-405 (1999).
[25] H.-Y. Chen, J. Wang, H. Yang, W.-Z. Li, H.-D. Li, "Synthesis of boron carbide films by ion beam sputtering", Surface and Coatings Technology **128-129**, 329-333 (2000).
[26] C. Ronning, D. Schwen, S. Eyhusen, U. Vetter, H. Hofsäss, "Ion beam synthesis of boron carbide thin films", Surface and Coatings Technology **158-159**, 382-387 (2002).
[27] R. Soufli, A. L. Aquila, F. Salmassi, M. Fernández-Perea, E. M. Gullikson, "Optical constants of magnetron sputtered boron carbide thin films from photoabsorption data in the range 30 to 770 eV", Appl. Opt. **47**, 4633-4639 (2008).
[28] D. G. Stearns, "A stochastic model for thin film growth and erosion," Appl. Phys. Lett. **62**(15), 1745-1747 (1993).
[29] E. Spiller, S. Baker, E. Parra, and C. Tarrio, "Smoothing of mirror substrates by thin film deposition," Proc. SPIE **3767**, 143-153 (1999).
[30] R. Soufli, E. Spiller, M. A. Schmidt, J. C. Robinson, S. L. Baker, S. Ratti, M. A. Johnson and E. M. Gullikson, "Smoothing of diamond-turned substrates for extreme-ultraviolet illuminators", Opt. Eng. **43**(12), 3089-3095 (2004).
[31] S. P. Hau-Riege, R.A. London, R.M. Bionta, D. Ryutov, R. Soufli, S. Bajt, M. A. McKernan, S. L. Baker , J. Krzywinski, R. Sobierajski, R. Nietubyc, J. B. Pelka, M. Jurek, L. Juha, J. Chalupský, J. Cihelka, V. Hájková, A. Velyhan, J. Krása, K. Tiedtke, S. Toleikis, H. Wabnitz, M. Bergh, C. Caleman, and N. Timneanu, "Wavelength dependence of the damage threshold of inorganic materials under extreme-ultraviolet free-electron-laser irradiation", submitted to App. Phys. Lett. (2009).
[32] S. P. Hau-Riege, R. A. London, R. M. Bionta, R. Soufli, D. Ryutov, M. Shirk, S. L. Baker, P. M. Smith, and P. Nataraj, "Multiple pulse thermal damage thresholds of materials for x-ray free electron laser optics investigated with an ultraviolet laser", Appl. Phys. Lett. **93**, 201105 (2008).
[33] A. Barty, R. Soufli, T. McCarville, S. L. Baker, M. J. Pivovaroff, P. Stefan and R. Bionta, "Predicting the coherent X-ray wavefront focal properties at the Linac Coherence Light Source (LCLS) X-ray free electron laser", submitted to Optics Express.